

General Rules for Predicting Where a Catalytic Reaction Should Occur on Metal Surfaces: A Density Functional Theory Study of C–H and C–O Bond Breaking/Making on Flat, Stepped, and Kinked Metal Surfaces

Zhi-Pan Liu and P. Hu*

Contribution from the School of Chemistry, The Queen's University of Belfast, Belfast BT9 5AG, United Kingdom

Received May 29, 2002; Revised Manuscript Received November 14, 2002 E-mail: p.hu@qub.ac.uk

Abstract: To predict where a catalytic reaction should occur is a fundamental issue scientifically. Technologically, it is also important because it can facilitate the catalyst's design. However, to date, the understanding of this issue is rather limited. In this work, two types of reactions, $\text{CH}_4 \leftrightarrow \text{CH}_3 + \text{H}$ and $\text{CO} \leftrightarrow \text{C} + \text{O}$ on two transition metal surfaces, were chosen as model systems aiming to address in general where a catalytic reaction should occur. The dissociations of $\text{CH}_4 \rightarrow \text{CH}_3 + \text{H}$ and $\text{CO} \rightarrow \text{C} + \text{O}$ and their reverse reactions on flat, stepped, and kinked Rh and Pd surfaces were studied in detail. We find the following: First, for the $\text{CH}_4 \leftrightarrow \text{CH}_3 + \text{H}$ reaction, the dissociation barrier is reduced by ~ 0.3 eV on steps and kinks as compared to that on flat surfaces. On the other hand, there is essentially no difference in barrier for the association reaction of $\text{CH}_3 + \text{H}$ on the flat surfaces and the defects. Second, for the $\text{CO} \leftrightarrow \text{C} + \text{O}$ reaction, the dissociation barrier decreases dramatically (more than 0.8 eV on Rh and Pd) on steps and kinks as compared to that on flat surfaces. In contrast to the $\text{CH}_3 + \text{H}$ reaction, the $\text{C} + \text{O}$ association reaction also preferentially occurs on steps and kinks. We also present a detailed analysis of the reaction barriers in which each barrier is decomposed quantitatively into a local electronic effect and a geometrical effect. Our DFT calculations show that surface defects such as steps and kinks can largely facilitate bond breaking, while whether the surface defects could promote bond formation depends on the individual reaction as well as the particular metal. The physical origin of these trends is identified and discussed. On the basis of our results, we arrive at some simple rules with respect to where a reaction should occur: (i) defects such as steps are always favored for dissociation reactions as compared to flat surfaces; and (ii) the reaction site of the association reactions is largely related to the magnitude of the bonding competition effect, which is determined by the reactant and metal valency. Reactions with high valency reactants are more likely to occur on defects (more structure-sensitive), as compared to reactions with low valency reactants. Moreover, the reactions on late transition metals are more likely to proceed on defects than those on the early transition metals.

1. Introduction

To predict where a catalytic reaction occurs, whether the reaction happens on flat surfaces or defects (such as steps and kinks), is very important as well as enormously challenging because of the following two reasons: Scientifically, it is one of the most fundamental issues in chemistry. Technologically, it has long been believed that the catalyst design would be tremendously aided once the reaction site is known. It has been observed that for some reactions the reaction rate changes dramatically with the catalyst structure; for example, the reaction rate increases significantly from single-crystal surfaces to small particles in which there are a large number of defects, while for other reactions, the reaction rate is independent of the catalyst structure. Qualitatively, two classes of catalytic processes have therefore been named: the structure-sensitive and structure-insensitive reactions.¹ With the aim to design the best catalyst,

the surface structure effect on reactions has been extensively studied over the past 40 years.^{1–24} To date, many observations have been reported. However, the understanding of the surface

- (2) (a) Somorjai, G. A. *J. Mol. Struct. (THEOCHEM)* **1998**, *424*, 101. (b) Somorjai, G. A. *Introduction To Surface Chemistry And Catalysis*; John Wiley & Sons Inc.: New York, 1994
- (3) Beebe, T. P., Jr.; Goodman, D. W.; Kay, B. D.; Yates, J. T., Jr. *J. Chem. Phys.* **1987**, *87*, 2305.
- (4) Lee, M. B.; Yang, Q. Y.; Tong, S. L.; Ceyer, S. T. *J. Chem. Phys.* **1987**, *87*, 2724.
- (5) Klier, K.; Hess, J. S.; Herman, R. G. *J. Chem. Phys.* **1997**, *107*, 10.
- (6) Wang, Y.-N.; Herman, R. G.; Klier, K. *Surf. Sci.* **1992**, *279*, 33.
- (7) Larsen, J. H.; Holmblad, P.; Chorkendorff, M. I. *J. Chem. Phys.* **1999**, *110*, 2637.
- (8) Wu, M.-C.; Goodman, D. W. *Surf. Sci. Lett.* **1994**, *306*, L529.
- (9) (a) Winters, H. F. *J. Chem. Phys.* **1975**, *62*, 2454. (b) Winters, H. F. *J. Chem. Phys.* **1976**, *64*, 3495.
- (10) Stewart, C. N.; Ehrlich, G. *J. Chem. Phys.* **1975**, *62*, 4672.
- (11) Rettner, C. T.; Pfnur, J. E.; Auerbach, D. *J. Phys. Rev. Lett.* **1985**, *54*, 2716.
- (12) Luntz, A. C.; Harris, J. *Surf. Sci.* **1991**, *258*, 397.
- (13) (a) Walker, A. V.; King, D. A. *J. Chem. Phys.* **2000**, *112*, 4739. (b) Juurlink, L. B. F.; McCabe, P. R.; Smith, R. R.; DiCologero, C. L.; Utz, A. L. *Phys. Rev. Lett.* **1999**, *83*, 868.
- (14) Jansen, A. P. J.; Burghraef, H. *Surf. Sci.* **1995**, *344*, 149.

(1) Boudart, M. *J. Mol. Catal.* **1985**, *30*, 27.

structure effect is rather limited. This is largely due to the difficulty to measure microscopic reaction pathways experimentally. In this paper, we report a detailed density functional theory (DFT) study on two fundamental processes, that is, C–H bond and C–O bond cleavage/formation, on flat, stepped, and kinked transition metal surfaces (Rh and Pd). With a careful examination of the calculated results, we have obtained an insight into where a catalytic reaction would occur on metal surfaces.

It has been long observed that the bond breaking processes in hydrocarbon conversion reactions are generally aided by corrugated surfaces; these reactions are structure-sensitive. In particular, kinks appear to be the most active sites for breaking any of the chemical bonds that are available during the hydrocarbon conversion reactions.² Taking the hydrogenolysis reaction that requires C–C bond scission as an example, we find that its reaction rate increases considerably (3- to 5-fold) when kinks are present in high concentrations on Pt surfaces.^{2b} The structure effect on methane decomposition ($\text{CH}_4 \rightarrow \text{CH}_3 + \text{H}$) was studied in detail by many surface science techniques.^{3–16} On Ni, Beebe et al. observed that Ni(110) is the best for CH_4 dissociation among Ni(111), Ni(100), and Ni(110). On Pd, Klier and co-workers^{5,6} reported that Pd(679), the surface with kinks, is the most active one; the reaction rate spans an order of magnitude in the order of $\text{Pd}(111) < \text{Pd}(311) < \text{Pd}(679)$. A summary of the surface structure effect on hydrocarbon conversion reactions can be found in the review article of Somorjai.^{2a}

Ammonia synthesis ($\text{N}_2 + \text{H}_2 \rightarrow \text{NH}_3$) on Fe, Ru-based catalysts was long observed to be very sensitive to the surface structure.^{17–20} Using STM and DFT calculations, Dahl et al.¹⁹ found that the N–N bond breaking on Ru(0001) is at least 9 orders of magnitude slower than that on steps. The reaction barrier on steps was calculated to be ~ 1.5 eV lower than that on flat surfaces.¹⁹ The same was also found for NO dissociation on Ru(0001).^{20,21} For N_2 and NO dissociation, DFT calculations showed that the transition state (TS) on monatomic steps involves five metal atoms, which is energetically more stable than the four-atom TS on close-packed surfaces. Hammer²⁵ suggested that the upshift of the d band on steps, that is, an electronic effect which helps to stabilize adsorbates, is the main reason for the barrier reduction in NO dissociation. However, Dahl et al. interpreted the large barrier reduction of N_2 dissociation on steps being mainly due to a geometrical effect on steps.^{19,20}

In contrast to the above structure-sensitive reactions, other reactions are quite inert to the change of surface structure, such as ethylene hydrogenation ($\text{CH}_2\text{CH}_2 + \text{H}_2 \rightarrow \text{CH}_3\text{CH}_3$) on metals. The reaction barriers for ethylene hydrogenation on a

series of Pt surfaces are similar, about 0.42 eV.¹ Ertl and Koch²² concluded that no crystal-plane specificity exists for steady-state CO oxidation on Pd at a temperature range of 300–900 K under low pressures. Recently, a surface science study by Uetsuka et al.²³ showed that the reaction rate of CO oxidation on Pd-steps (Pd(335)) is slightly faster (about 1.5 times) than that on (111) terraces. They found that CO oxidation switches from steps to terraces when the CO coverage is varied. In line with this, DFT calculations of Zhang and Hu²⁵ showed that for CO oxidation on Pd(111), the reaction barrier is strongly affected by the CO coverage, and the reaction is structure-insensitive at medium CO coverage. On Pt(111), the CO coverage dependency for CO oxidation was also found.¹

To date, no general framework has been established to understand the surface structure effect, and many puzzles regarding the reactivity of different sites for different reactions have not been rationalized. In particular, the following question remains to be answered: Where is the favored site for a particular reaction? This question can be rephrased as follows: (i) What kind of reaction may be structure-sensitive and why? (ii) Is the structure-sensitivity metal-dependent? If it is, what is the reason? To answer these questions, in this work we have chosen two elementary reactions, $\text{CH}_4 \leftrightarrow \text{CH}_3 + \text{H}$ and $\text{CO} \leftrightarrow \text{C} + \text{O}$, on two transition metal surfaces (Rh and Pd) as probes to tackle the surface structure effect. For each reaction, different reaction sites, that is, flat (111) face, stepped, and kinked Rh and Pd surfaces were studied. These model systems were selected on the basis of two reasons. Technologically, they are elementary steps in many important processes, such as methane activation and Fischer–Tropsch reactions. Scientifically, they are relatively simple and can thus be considered as prototypical reactions in heterogeneous catalysis. In addition, it should be mentioned that the flat (111) surface (of fcc metal) is close-packed and thus the dominant face in real catalysts, and steps and kinks are perhaps the most common defects.

Our DFT calculations show that *surface defects, especially the steps, are generally favored for bond-breaking reactions*, while the association reaction (bond making) can be either structure-sensitive or -insensitive, depending on *individual reactions* as well as *the particular metal*. Physical origins of these trends are identified and discussed. Although only two types of reactions on Rh and Pd were tackled in this study, the understanding we have obtained is of general chemical interest. This paper is organized as follows: The calculation methods are described in section 2. In section 3, calculation results, that is, the reaction pathways and energetics for $\text{CH}_4 \leftrightarrow \text{CH}_3 + \text{H}$ and $\text{CO} \leftrightarrow \text{C} + \text{O}$ on flat surfaces, steps, and kinks, are reported. Their transition state geometries are compared and discussed. In section 4, we discuss the origin of the surface structure effect on these reactions. In the last section, conclusions are summarized.

2. Calculation Methods

Density functional theory calculations with the generalized gradient approximation²⁶ were performed. The electronic wave functions were expanded in a plane wave basis set, and the ionic cores were described by ultrasoft pseudopotentials.²⁷ The vacuum region between slabs was

- (15) Mortensen, H.; Diekhöner, L.; Baurichter, A.; Luntz, A. C. *J. Chem. Phys.* **2002**, *116*, 5781.
- (16) Egeberg, E. C.; Ullmann, S.; Alstrup, I.; Mullins, C. B.; Chorkendorff, I. *Surf. Sci.* **2002**, *497*, 183.
- (17) Ertl, G. In *Catalytic Ammonia Synthesis*; Jennings, J. R., Ed.; Plenum Press: New York, 1991; p 109.
- (18) Dahl, S.; Tornqvist, Jacobsen, C. J. H. *J. Catal.* **2001**, *198*, 97.
- (19) Dahl, S.; Logadottir, A.; Egeberg, R. C.; Larsen, J. H.; Chorkendorff, I. *Phys. Rev. Lett.* **1999**, *83*, 1814.
- (20) Dahl, S.; Tornqvist, E.; Chorkendorff, I. *J. Catal.* **2000**, *192*, 381.
- (21) Zambelli, T.; Wintterlin, J.; Trost, J.; Ertl, G. *Science* **1996**, *273*, 1688.
- (22) Hammer, B. *Phys. Rev. Lett.* **1999**, *83*, 3681.
- (23) Ertl, G.; Koch, J. In *Proceedings of the 5th International Congress on Catalysis*; Hightower, J., Ed.; North-Holland: Amsterdam, 1973; p 969.
- (24) Uetsuka, H.; Watanabe, K.; Kimpura, Kunimori, K. *Langmuir* **1999**, *15*, 5795.
- (25) Zhang, C. J.; Hu, P. *J. Am. Chem. Soc.* **2001**, *123*, 1166.

- (26) (a) Perdew, J. P.; Chevary, J. A.; Vosko, S. H.; Jackson, K. A.; Pederson, M. R.; Singh, D. J.; Fiolhais, C. *Phys. Rev. B* **1992**, *46*, 6671. (b) Lynch, B. J.; Fast, P. L.; Harris, M.; Truhlar, D. G. *J. Phys. Chem.* **2000**, *104*, 4811.

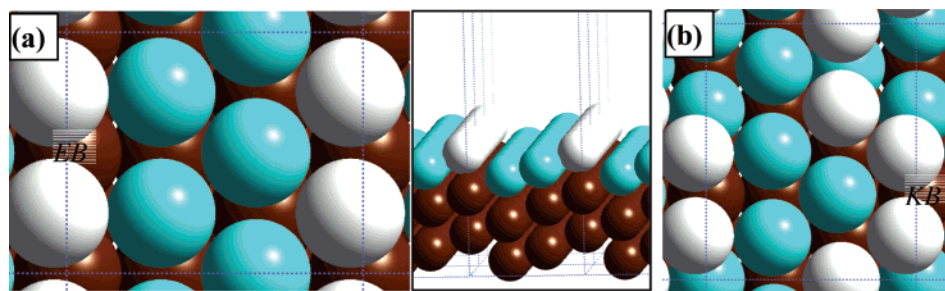


Figure 1. Illustration of the geometrical structures of calculated Rh-step and Rh-kink (the Pd-step and the Pd-kink studied are similar to the Rh counterpart in this figure). (a) The top view (left) and side view (right) of Rh-step, which is a Rh(211) surface; the dotted line shows the (1×2) unit cell of Rh(211). The step-edge Rh atoms are white balls. EB labels the step-edge bridge site. (b) The top view of Rh-kink, which is constructed by taking one step-edge Rh atom from the (1×3) unit cell of Rh(211). KB labels the kink-edge bridge site.

10 Å, and a cutoff energy of 340 eV was used. Monkhorst–Pack k-point sampling with 0.07 \AA^{-1} spacing was utilized for all of the calculations (for example, for a $p(2 \times 2)$ Rh(111) slab, $3 \times 3 \times 1$ k-point sampling is used).

To fully compare the reactivity of flat and corrugated surfaces for a reaction, we have modeled the flat surfaces, Rh(111) and Pd(111), using large unit cells that correspond to the low coverage of reactions. The $\text{CH}_4 \leftrightarrow \text{CH}_3 + \text{H}$ reactions were performed in the $p(2 \times 5)$ unit cell ($1/10$ monolayer (ML)) with four layers, and the $\text{CO} \leftrightarrow \text{C} + \text{O}$ reactions were in the $p(3 \times 3)$ unit cell ($1/9$ ML) with three layers. We found that for $\text{CH}_4 \leftrightarrow \text{CH}_3 + \text{H}$ reactions, the coverage effect on the dissociation barriers is very small (below 0.1 eV), and for $\text{CO} \leftrightarrow \text{C} + \text{O}$ reactions, the coverage effect is about 0.1 eV. All of the flat surfaces were fixed at the bulk-truncated structures because the surface relaxations of Rh(111) and Pd(111) have a very small effect on the reaction barriers (below 0.1 eV) when the large unit cells are used. We have checked the barrier of CH_4 dissociation on a series of Rh(111) slabs in detail; see ref 28. The zero point energy is not included.

The Rh-step and the Pd-step were modeled by (1×2) unit cells ($1/6$ ML) of Rh(211) and Pd(211), respectively (see Figure 1a). The (211) surface contains steps of (100)-type, which is found to be more active than the (111)-type step in catalytic reactions.²¹ The kinked surfaces were constructed by removing one edge atom at the step in a (1×3) unit cell of the (211) surface (see Figure 1b). Hereafter, the kinked surfaces obtained from Rh(211) and Pd(211) are named as the Rh-kink and the Pd-kink, respectively. All of the corrugated surfaces were modeled with “effective” three layers (see Figure 1a, side view) with the top layer being relaxed and the other layers being fixed at the bulk-truncated structure. It should be mentioned that the least coordination number (CN) of metal atoms on these surfaces is different: It reduces from the flat surfaces to the steps and to the kinks, for example, on Rh(111) CN = 9, on Rh-steps CN = 7 (the metal atom of the EB site, Figure 1a), and on Rh-kinks CN = 6 (the metal atom of the KB site, Figure 1b). TSs of reactions were searched using a constrained minimization technique. The TS was identified when (i) the force on the atoms vanish and (ii) the energy is a maximum along the reaction coordinate, but a minimum with respect to all of the remaining degrees of freedom. Our previous work has demonstrated that the above DFT setup affords a good accuracy, especially for the calculation of reaction barriers in heterogeneous catalysis.^{29–34} As compared to the experi-

mental values, the error in our calculated barriers is around 0.1 eV. It should be mentioned that the error in barriers from DFT-GGA could, in general, be higher.^{26b}

3. Results and Discussions

3.1. $\text{CH}_4 \leftrightarrow \text{CH}_3 + \text{H}$ on Flat and Corrugated Surfaces.

Being the essential step for methane conversion, $\text{CH}_4 \rightarrow \text{CH}_3 + \text{H}$ on metals has been a hot subject focused by many experimental and theoretical studies over the last several decades. The general consensus obtained from experiments can be summarized as follows: (i) Over transition metal surfaces, CH_4 dissociation occurs at relatively low temperatures, even on Pd (400 K); (ii) the process is assisted by the vibrational energy of methane;¹³ and (iii) the apparent activation energies are low, but the reactive sticking probabilities are also low. On several close-packed metal surfaces, such as Ni(111), Ru(0001), and Pd(111), the apparent CH_4 dissociation barriers (E_a^{eff}) have been measured experimentally. On Ni(111), E_a^{eff} is about 0.55 eV, reported by Beebe et al. and Ceyer et al.;^{3,4} on Ru(0001), $E_a^{\text{eff}} \approx 0.37$ eV by Wu et al.;⁸ on Pd(111), $E_a^{\text{eff}} \approx 0.33$ eV by Klier et al.^{5,6} As mentioned in the Introduction, CH_4 dissociation was found to be structure-sensitive. On corrugated surfaces, it is generally faster than that on flat surfaces. Theoretically, CH_4 dissociation on Ni(111) and Ru(0001) has been calculated using DFT. Two groups have reported similar barriers for CH_4 dissociation on Ni(111), ~ 0.8 eV,^{35,36} while the others³⁷ reported even higher barriers. Ciobica et al.³⁸ obtained a barrier of 0.88 eV for methane dissociation on Ru(0001), and it was calculated to be 0.79 eV by us.

When comparing the experimental values to the DFT barriers, it is quite surprising to find that the barriers obtained from DFT calculations are generally several tenths of an eV (0.3–0.4 eV) larger than the measured barriers. The reason for this inconsistency is unknown yet. Two possibilities might be involved: (i) In real systems, CH_4 dissociation may not occur on the flat

(27) Vanderbilt, D. *Phys. Rev. B* **1990**, *41*, 7892.

(28) The barrier (E_a^{dis}) of CH_4 dissociation on a series of Rh(111) slabs is shown as follows (the E_a^{dis} reported in Table 3 corresponds to the one labeled with *):

Unit cell	Layers	Top layer	E_a^{dis} (eV)
p(2x2)	3	fixed	0.77
p(2x2)	3	relaxed	0.72
p(2x2)	4	relaxed	0.62
p(2x3)	3	fixed	0.67
p(2x3)	4	relaxed	0.61
p(2x5)	4	fixed	0.67*

(29) Liu, Z.-P.; Hu, P. *J. Am. Chem. Soc.* **2001**, *123*, 12596.

(30) (a) Liu, Z.-P.; Hu, P. *J. Chem. Phys.* **2001**, *114*, 8244. (b) Liu, Z.-P.; Hu, P. *J. Chem. Phys.* **2001**, *115*, 4977.

(31) Liu, Z.-P.; Hu, P. *J. Am. Chem. Soc.* **2002**, *124*, 5175. Liu, Z.-P.; Hu, P.; Alavi, A. *J. Chem. Phys.* **2001**, *114*, 5956.

(32) Zhang, C. J.; Hu, P. *J. Am. Chem. Soc.* **2000**, *122*, 2134. Zhang, C. J.; Hu, P.; Alavi, A. *J. Am. Chem. Soc.* **1999**, *121*, 7931. Zhang, C. J.; Liu, Z.-P.; Hu, P. *J. Chem. Phys.* **2001**, *114*, 8244.

(33) Michaelides, A.; Hu, P. *J. Am. Chem. Soc.* **2001**, *123*, 4235. Michaelides, A.; Hu, P. *J. Am. Chem. Soc.* **2000**, *122*, 9866. Michaelides, A.; Hu, P. *J. Chem. Phys.* **2001**, *114*, 5792. Michaelides, A.; Hu, P. *J. Chem. Phys.* **2001**, *115*, 8570.

(34) Sachs, C.; Hildebrand, M.; Volkening, S.; Winterlin, J.; Ertl, G. *Science* **2001**, *293*, 1635.

(35) Yang, H.; Whitten, J. L. *J. Chem. Phys.* **1992**, *96*, 5529.

(36) Michaelides, A.; Hu, P.; Alavi, A. *J. Chem. Phys.* **1999**, *111*, 1343.

(37) Kratzer, P.; Hammer, B.; Norskov, J. K. *J. Chem. Phys.* **1996**, *105*, 5595.

(38) Ciobica, I. M.; Frechard, F.; van Santen, R. A.; Kleyn, A. W.; Hafner, J. *J. Phys. Chem. B* **2000**, *104*, 3364.

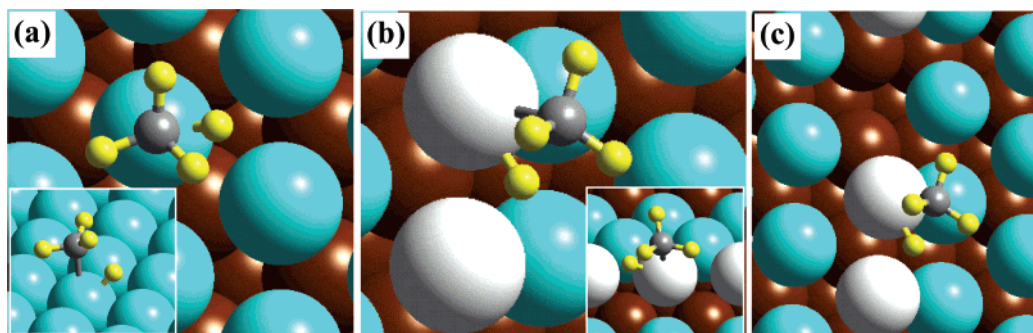


Figure 2. The top view of the calculated TS structures for $\text{CH}_4 \leftrightarrow \text{CH}_3 + \text{H}$ reactions on Rh(111) (a), Rh-step (b), and Rh-kink (c). Side views of the TSs on the Rh(111) and the Rh-step are shown in insets in (a) and (b), respectively. The TSs for $\text{CH}_4 \leftrightarrow \text{CH}_3 + \text{H}$ on Pd surfaces are similar. The small gray balls, small yellow balls, and big balls are C atoms, H atoms, and Rh atoms, respectively. In particular, the step-edge Rh atoms in the Rh-step and the Rh-kink are shown as big white balls.

Table 1. The CH_3 and H Atom Adsorption Energies (E_{ad}) and the Adsorption Sites on Different Rh and Pd Surfaces (the Final State for CH_4 Dissociation)^a

	CH_3			H	
	E_{ad}	site	$d_{\text{C-metal}}$ (Å)	E_{ad}	site
Rh(111)	1.88	fcc	2.262		
Rh-step	2.16	EB	2.078, 2.344	2.92	fcc
Rh-kink	2.16	KB	2.100, 2.362		
Pd(111)	1.78	top	2.058		
Pd-step	2.01	EB	2.117, 2.278	3.05	fcc
Pd-kink	1.88	KB	2.195, 2.182		

^a The structures of the step and the kink and chemisorption sites (EB, KB) are shown in Figure 1. The distances for the CH_3 to its nearest-neighbor metal atoms ($d_{\text{C-metal}}$) are also listed. For the H atom, its adsorption energies on flat surfaces, steps, and kinks are very similar (within 0.05 eV), and thus the E_{ad} on the flat surfaces is used for all of the surfaces.

surfaces, but on a small number of defects. As shown in the recent experiment of Dahl et al., N_2 dissociation on Ru(0001) is in fact totally dominated by a small number of steps. Whether CH_4 dissociation also follows such a scenario is not certain. (ii) A quantum-mechanical tunneling mechanism, suggested by Winters,⁹ might exist, which largely reduces the effective barrier obtained from experiments. To date, no theoretical calculations were reported for CH_4 dissociation on corrugated surfaces, and possibility (i) therefore could not be ruled out. With the aim to elucidate the above puzzle and shed light on the structure-sensitivity of methane dissociation, we have investigated CH_4 dissociation on flat (111), stepped (211), and kinked Rh and Pd surfaces.

3.1.1. CH_3 and H Atom Adsorption. As a starting point, the chemisorption energies (E_{ad}) of CH_3 and the H atom on all of the surfaces, that is, the flat surfaces, the steps, and the kinks, were calculated. Together with the optimized metal– CH_3 distances, the E_{ad} 's are listed in Table 1. On both flat Rh(111) and flat Pd(111), the H atom is the most stable at the fcc hollow site (Rh(111), $E_{\text{ad}}(\text{H}) = 2.92$ eV; Pd(111), $E_{\text{ad}}(\text{H}) = 3.05$ eV). The potential energy surface of CH_3 is quite flat on both metals; CH_3 slightly prefers the fcc hollow site on Rh(111) ($E_{\text{ad}}(\text{CH}_3) = 1.88$ eV, 0.12 eV more stable than that on a top site); it preferably sits on the top site on Pd(111) ($E_{\text{ad}}(\text{CH}_3) = 1.78$ eV, 0.08 eV more stable than that on a fcc hollow site), which is consistent with the previous calculation of Paul and Sautet.³⁹ Other DFT studies showed that on Ni(111),⁴⁰ Cu(111),⁴¹ and

Table 2. The Important Structural Parameters (Distances, d , Angle, \angle) for the TSs of $\text{CH}_4 \leftrightarrow \text{CH}_3 + \text{H}$ on Different Rh and Pd Surfaces^a

	$\text{CH}_4 \leftrightarrow \text{CH}_3 + \text{H}$			
	$d_{\text{C-metal}}$ (Å)	$d_{\text{H-metal}}$ (Å)	$d_{\text{C-H}}$ (Å)	$\angle(\text{C-metal-H})$ (deg)
Rh(111)	2.206	1.667, 2.074, 2.246	1.550	44.5
Rh-step	2.168	1.682, 1.929	1.544	45.1
Rh-kink	2.140	1.703, 1.882	1.573	46.6
Pd(111)	2.157	1.695, 2.006, 2.106	1.540	45.2
Pd-step	2.155	1.676, 1.839	1.595	47.2
Pd-kink	2.120	1.668, 1.783	1.691	51.3

^a The TSs are shown in Figure 2. H_a is the reacting H atom in $\text{CH}_4 \leftrightarrow \text{CH}_3 + \text{H}$.

Ru(0001),³⁸ CH_3 sits on the hollow site, while on 5d metal, for example, Pt(111),⁴¹ it is on the top site.

On all of the corrugated surfaces, that is, steps and kinks, the most stable chemisorption site for CH_3 is always the bridge site of the step-edge (EB site or KB site in Figure 1). Generally, the steps improve the CH_3 chemisorption energy by several tenths of an eV as compared to the flat surfaces, while there is no further energy gain when the CH_3 shifts from the steps to the kinks. For example, $E_{\text{ad}}(\text{CH}_3)$ is 2.16 eV on both Rh-step and Rh-kink, and this value is 0.28 eV higher than that on Rh(111). It is interesting to note that the H atom adsorption is insensitive to the surface change: The difference between the calculated $E_{\text{ad}}(\text{H})$ on the steps and kinks and that on the flat surfaces is less than 0.05 eV. Thus, we take the H atom at the flat surfaces as the final state (FS) of the H atom after CH_4 dissociation.

3.1.2. Reaction Pathways and Barriers of $\text{CH}_4 \leftrightarrow \text{CH}_3 + \text{H}$. On flat Rh(111) and Pd(111), CH_4 dissociation occurs over a top site of a metal atom. Figure 2a shows the located TS geometry on Rh(111) (the TS on Pd(111) is similar). At the TS, the CH_3 sits on the top site, and the activated H atom is near a fcc hollow site. The important TS structural parameters are listed in Table 2. This TS structure is similar to previous results for CH_4 dissociation on other close packed surfaces, for example, Ni(111), Pt(111), and Ru(0001). Here we summarize two general features of the TS of methane dissociation on these surfaces. First, the TSs belong to “late TSs” (close to the final state). This is evident from the located TS structures: (i) The H– CH_3 bonds at the TSs are well stretched as compared to the C–H bond length of methane (1.5–1.6 Å at the TSs (Table 2) and 1.08 Å in the CH_4 molecule). (ii) The metal– CH_3 and metal–H bond distances are rather short and close to the

(39) Paul, J.-F.; Sautet, P. *J. Phys. Chem. B* **1998**, *102*, 1578.

(40) Yang, H.; Whitten, J. L. *J. Am. Chem. Soc.* **1991**, *113*, 6442.

(41) Michaelides, A.; Hu, P. *J. Chem. Phys.* **2001**, *114*, 2523.

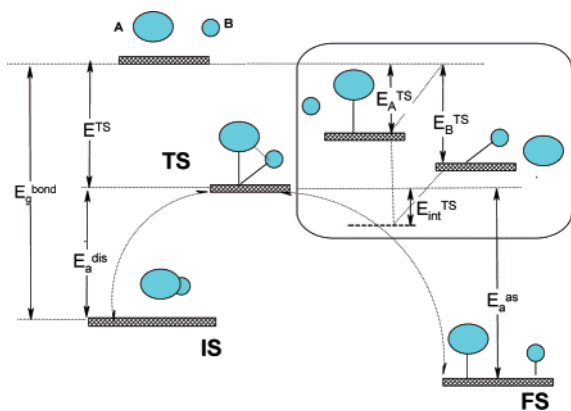


Figure 3. The energetic diagram for a general $AB \rightarrow A + B$ reaction on metal surfaces. The inset shows the energy decomposition of the TS total chemisorption energy (E^{TS}) at TS. All of the terms are defined and discussed in the text.

optimized distances of the individual CH_3 and H adsorption, respectively. For example, the optimized Rh– CH_3 bond length (CH_3 sitting at a top site) is 2.107 Å, while the Rh– CH_3 distance at the TS is 2.206 Å (Table 2). It should be mentioned that the late TS of methane dissociation is consistent with the experiment that CH_4 dissociation is assisted by vibrational energies. Second, each TS mainly involves one metal atom, on which the CH_3 sits. The H atom, although near the fcc hollow site, does not bond with the other two surface atoms strongly, as is evident from the distances of the H atom to the three metal atoms at the TS (Table 2).

We then located the most stable TSs for CH_4 dissociation on steps, the Rh-step and the Pd-step (see Figure 1a) and kinks, the Rh-kink and the Pd-kink (shown in Figure 1b, see Calculation Methods). Figure 2b and c shows the TSs for CH_4 dissociation on the Rh-step and the Rh-kink (the TSs on the Pd-step and the Pd-kink are similar to the Rh counterparts). As can be seen from Figure 2b and c, the TSs on the steps and the kinks in fact are very similar: Both locate at the step-edge, in which CH_3 sits on the top site of one edge metal atom, and the H atom is near the bridge site of the step-edge. The important TS structural parameters on the steps and the kinks are listed in Table 2, together with those on the flat surfaces. With a careful comparison, we found that the TSs on the steps and the kinks share the same basic features with the TS on the flat surfaces (Figure 2a). The TSs on the steps and the kinks also (i) belong to late TSs and (ii) mainly involve one metal atom. In fact, the TSs on the steps and the kinks may be even “later”. This is reflected in the longer H– CH_3 distances at the TSs. For instance, at the TS on the Pd-step, $d_{\text{H-CH}_3}$ is 1.595 Å; on the Pd-kink, it is 1.691 Å, as compared to 1.540 Å on Pd(111).

With all of the states being determined, we then calculated the dissociation barrier (E_a^{dis}) for $\text{CH}_4 \rightarrow \text{CH}_3 + \text{H}$ as well as the association barrier (E_a^{as}) for the reverse reaction, $\text{CH}_3 + \text{H} \rightarrow \text{CH}_4$. Figure 3 illustrates in general all of the energy terms used in Table 3 for a dissociation reaction and the reverse reaction. E_a^{as} is 0.59 eV on Rh(111) and 0.62 eV on Pd(111). It is noticed that the reaction energies (ΔH , the energy difference between the initial state (IS) and the FS, $\Delta H = E_a^{\text{as}} - E_a^{\text{dis}}$, see Figure 3) are almost zero for $\text{CH}_4 \leftrightarrow \text{CH}_3 + \text{H}$ on Rh(111) and Pd(111). On the steps and the kinks, we found that the E_a^{dis} decreases considerably: $E_a^{\text{dis}} = 0.32$ eV on the Rh-step and 0.20 eV on the Rh-kink; $E_a^{\text{dis}} = 0.38$ eV on the Pd-step and

Table 3. The Calculated Dissociation Barriers (E_a^{dis}) for $\text{CH}_4 \rightarrow \text{CH}_3 + \text{H}$ and $\text{CO} \rightarrow \text{C} + \text{O}$ and the Barriers (E_a^{as}) for Their Reverse Reactions on Different Rh and Pd Surfaces^a

	$\text{CH}_4 \leftrightarrow \text{CH}_3 + \text{H}$		$\text{CO} \leftrightarrow \text{C} + \text{O}$		CN
	E_a^{dis}	E_a^{as}	E_a^{dis}	E_a^{as}	
Rh(111)	0.67	0.65	1.17	1.84	9
Rh-step	0.32	0.59	0.30	1.18	7
Rh-kink	0.20	0.49	0.21	1.09	6
Pd(111)	0.66	0.68	1.87	1.98	9
Pd-step	0.38	0.63	0.57	0.68	7
Pd-kink	0.41	0.53	0.38	0.49	6

^a The least coordination number (CN) of the metal atoms involved in the TSs on flat surfaces, steps, and kinks are also listed for comparison. The unit of the barriers is eV.

0.41 eV on the Pd-kink. However, E_a^{as} of the $\text{CH}_3 + \text{H}$ reaction on the steps is similar to that on the flat surfaces, and they only decrease by ~ 0.1 eV if the reaction occurs on the kinks (Table 3).

3.1.3. Discussion of the Reaction Mechanism of $\text{CH}_4 \leftrightarrow \text{CH}_3 + \text{H}$ on Transition Metals. As mentioned before, for CH_4 dissociation on close-packed surfaces, for example, Ni(111) and Ru(0001), the barriers calculated from DFT are about 0.3 eV larger than the values measured experimentally. This is also true on Pd(111), as we compared our calculated barrier for CH_4 dissociation on Pd(111) (0.67 eV) to the value recently reported by Klier et al. (0.36 eV (34.3 kJ/mol)). However, we found interestingly that for the barriers on the steps and the kinks, the consistency between our results and the experimental ones reported by Klier et al. is very good. The effective barriers for methane dissociation on Pd(311) (with steps) and Pd(679) (with kinks) are 0.33 eV (32.2 kJ/mol) and 0.44 eV (43.9 kJ/mol), respectively, and our calculated ones are 0.38 eV on Pd-steps and 0.41 eV on Pd-kinks. In addition, our barriers on the step and the kink of Rh (0.2–0.3 eV) are in good agreement with the early experiment work of Ehrlich et al.,¹⁰ who reported the barrier of methane dissociation on Rh films being ~ 0.3 eV.

To reconcile the above puzzle, we have done the following analysis on the reaction rate. Using the Arrhenius equation, we estimated the initial sticking coefficients (S_0) as

$$S_0 \approx A \exp(-E_a/RT)[\text{sites}]$$

where T is assumed to be 500 K, A is the preexponential factor, and [sites] is the concentration of reaction sites. A small change in E_a will lead to a large change in reaction rate (S_0); a 0.3 eV change in E_a (e.g., CH_4 dissociation goes from flat surfaces to steps) will lead to S_0 differing by 10^3 if everything else is the same. Even assuming the population of the stepped sites is only 1% of the flat surface sites and A is constant, we find that the S_0 on steps (S_0^{step}) is still ~ 10 times larger than S_0 on flat surfaces (S_0^{flat}). Therefore, the overall S_0 is dominated by S_0^{step} , and the effective barrier E_a^{eff} would be largely determined by E_a^{dis} on steps. This means that the measured E_a^{eff} would correspond to E_a^{dis} on steps, which is ~ 0.3 eV smaller than the E_a^{dis} on flat surfaces. Therefore, this indicates that the CH_4 dissociation reaction should be structure-sensitive (Table 2). On the other hand, a barrier decrease of 0.1–0.2 eV can only increase $\exp(-E_a/RT)$ by 10–100 times at 500 K, which is likely to be tempered by the number of the active sites. This suggests that the $\text{CH}_3 + \text{H}$ association is largely structure-insensitive because its barrier (E_a^{as}) variation is small (Table 2).

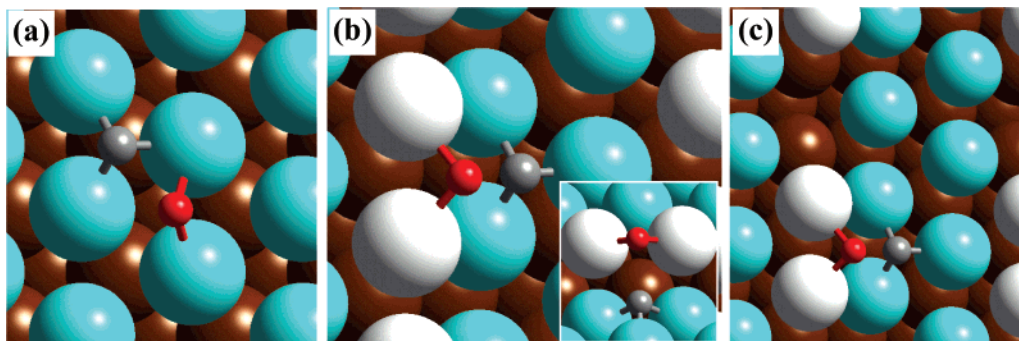


Figure 4. The top view of the calculated TS structures for $\text{CO} \leftrightarrow \text{C} + \text{O}$ reactions on Rh(111) (a), Rh-step (b), and Rh-kink (c). The side view of the TS on the Rh-step is shown in the inset in (b). The TSs for $\text{CO} \leftrightarrow \text{C} + \text{O}$ on Pd surfaces are similar to those on Rh. The small gray balls, small red balls, and big balls are C atoms, O atoms, and Rh atoms, respectively. In particular, the step-edge Rh atoms in the Rh-step and the Rh-kink are shown as big white balls.

On the basis of these results, we suggest that *CH₄ dissociation even on single crystal surfaces may be dominated by a small number of defects, especially steps*, considering that steps always exist on single crystal surfaces. Kinks may not play an important role due to their much smaller population than steps and the similar reactivity with steps. This suggestion can be used to reconcile the puzzle mentioned before. The experimentally measured barrier for CH_4 dissociation on Pd(111) is lower (0.3 eV) than the calculated one on the flat surface, but is very close to that calculated on the steps and the kinks. Moreover, the population of stepped sites on a surface is expected to be the controlling factor to the reaction rate. This is indeed what was observed experimentally. Klier et al. found that CH_4 dissociation on Pd(679) is about 10 times faster than that on Pd(111), the magnitude of which is consistent with the difference of the step population between two surfaces: 13% of Pd(679) are steps, while there are at least 1% steps on Pd(111). It should be mentioned that on the basis of our calculations, we believe that the tunneling effect in CH_4 dissociation might not be very crucial, which was also suggested in a recent paper.¹⁵

It is worth mentioning some nice experiment work of Egeberg et al.,¹⁶ which was just published very recently. Egeberg et al. carefully studied the dissociation of CH_4 on Ni(111) and Ru(0001) to examine whether the stepped sites have a large effect on CH_4 dissociation. They reported that sputtering of the Ni(111) surface without subsequent annealing was found to increase the initial sticking by 2–5 times, while the Ru(0001) deposited by a small amount of Au (Au was observed to occupy the stepped sites) slightly reduces the initial sticking. These new experimental results are consistent with our discussions above. It is interesting to address the reason for the little effect of the Au deposition on CH_4 dissociation, as compared to its large effect on N_2 dissociation (the deposition of Au on Ru(0001) dramatically increases the N_2 dissociation barrier from 0.4 to 1.5 eV¹⁹). This can be readily explained by our DFT calculations: The TS of CH_4 dissociation only involves one metal atom (even on steps), which is different from the TS of N_2 dissociation (involving the five-atom on steps). Therefore, the Au deposition could not block the dissociation site of CH_4 dissociation on steps (may have some electronic effect, see discussion in section 4), but completely blocks that of N_2 dissociation (also see section 4).

As mentioned before, our calculation results show that the reverse reaction of CH_4 dissociation, $\text{CH}_3 + \text{H} \rightarrow \text{CH}_4$, is quite inert to the structure change. One piece of evidence to support the C–H bond formation being structure-insensitive is that the

ethylene hydrogenation ($\text{CH}_2=\text{CH}_2 + \text{H}_2 \rightarrow \text{CH}_3-\text{CH}_3$) reactions on Pt and Rh were found to be structure-insensitive.

3.2. CO \leftrightarrow C + O on Flat and Corrugated Surfaces. Using syngas (CO and H_2) to produce hydrocarbons is one of the most important industrial processes in heterogeneous catalysis. CO dissociation ($\text{CO} \rightarrow \text{C} + \text{O}$), which produces the active surface carbons, appears to be an essential step for CH_4 formation ($\text{CO} + 3\text{H}_2 \rightarrow \text{CH}_4 + \text{H}_2\text{O}$) and a Fischer–Tropsch reaction ($n\text{CO} + 2n\text{H}_2 \rightarrow \text{C}_n\text{H}_{2n} + n\text{H}_2\text{O}$, $n > 2$).² CO dissociative adsorption is commonly observed on Ru, Co, Rh, Ni metals (500 K), while CO appears to adsorb only molecularly on late 4d, 5d metals, such as Pd, Ir, and Pt. However, it was found experimentally that on late 4d, 5d metals, CH_4 is also produced from CO and H_2 .^{42–44} Pichler and Emmett⁴⁵ proposed a mechanism to explain this puzzle, involving the direct hydrogenation of molecular CO . In the last several years, using STM technique and DFT calculations, many workers^{18–22} showed that the dissociation of some diatomic molecules, such as N_2 and NO , is dominated by the steps of metals. Thus, one may speculate that CO dissociation is also likely to follow the same mechanism on late 4d and 5d metals: It occurs on steps, where the reaction is much easier as compared to that on flat surfaces. In the following subsection, we will examine this possibility.

3.2.1. Reaction Pathways and Barriers of CO \leftrightarrow C + O on Flat Surfaces. We have calculated $\text{CO} \leftrightarrow \text{C} + \text{O}$ on a series of flat 4d and 5d close-packed surfaces, that is, Ru(0001), Rh(111), Pd(111), Os(0001), Ir(111), and Pt(111) at $1/4$ ML coverage previously (see ref 30b). We have shown that on these surfaces, the TSs of CO dissociation are similar: They are all late TSs. In addition to the previous work, in this work we have recalculated CO dissociation at a low coverage on Rh(111) and Pd(111), $1/9$ ML ($p(3 \times 3)$ unit cell), to better compare the reactivity between different surface structures (the decrease of coverage will change the barriers slightly because the TS and the FS are more stable at low coverages; for example, the CO dissociation barrier on Rh(111) at $1/4$ ML is 1.25 eV, and it is 1.17 eV at $1/9$ ML). Figure 4a shows the TS structure for CO dissociation on Rh(111) (the TS on Pd(111) is similar). At the TS, the C atom is near the hcp hollow site, and the O atom is close to a bridge site. The important TS structural parameters are listed in Table 4. It appears that at the TS, four surface atoms

(42) Rabo, J. A.; Risch, A. P.; Poutsma, M. L. *J. Catal.* **1978**, *53*, 295.

(43) Poutsma, M. L.; Elek, L. F.; Ibarbia, P.; Risch, H.; Babo, J. A. *J. Catal.* **1978**, *52*, 157.

(44) Vannice, M. A. *Catal. Rev. Sci. Eng.* **1976**, *14*, 153.

(45) Hall, W. K.; Kokes, R. J.; Emmett, P. H. *J. Am. Chem. Soc.* **1960**, *82*, 1027. Pichler, H. *Adv. Catal. Relat. Subj.* **1952**, *4*, 271.

Table 4. The Important Structural Parameters (Distances, d) for the TSs of $\text{CO} \leftrightarrow \text{C} + \text{O}$ on Different Rh and Pd Surfaces^a

	$\text{CO} \leftrightarrow \text{C} + \text{O}$		
	$d_{\text{C-metal}}$	$d_{\text{O-metal}}$	$d_{\text{C-O}}$
Rh(111)	1.890, 1.959, 2.029	2.046, 2.145	1.865
Rh-step	1.904, 1.943, 1.943	1.966, 1.966	2.090
Rh-kink	1.911, 1.947, 1.947	1.975, 1.975	2.090
Pd(111)	1.885, 1.935, 2.019	2.009, 2.136	1.980
Pd-step	1.859, 1.897, 1.897	1.930, 1.930	2.724
Pd-kink	1.886, 1.886, 1.901	1.931, 1.931	2.500

^a The TSs are shown in Figure 4. In all of the TS structures, the C atom is on the three-fold hollow site, and the O atom is on the bridge site (see Figure 4a–c).

are directly involved in bonding with the TS complex, one of the surface atom being shared by the C and the O. After CO dissociation, the C atom prefers a hcp hollow site, and the O atom favors a fcc hollow site on both Rh(111) and Pd(111). The calculated adsorption energies (E_{ad}) at $1/9$ ML are as follows: on Rh(111), $E_{\text{ad}}(\text{C}) = 7.12$ eV and $E_{\text{ad}}(\text{O}) = 4.78$ eV, and on Pd(111), $E_{\text{ad}}(\text{C}) = 6.85$ eV and $E_{\text{ad}}(\text{O}) = 4.39$ eV. The dissociation barriers ($E_{\text{a}}^{\text{dis}}$) and the association barriers of $\text{CO} \leftrightarrow \text{C} + \text{O}$ were calculated and listed in Table 3, together with those of the $\text{CH}_4 \leftrightarrow \text{CH}_3 + \text{H}$ reaction.

3.2.2. Reaction Pathways and Barriers of $\text{CO} \leftrightarrow \text{C} + \text{O}$ on Steps and Kinks. We then investigated CO dissociation on the Rh-step, the Pd-step, the Rh-kink, and the Pd-kink. CO dissociation on these defects possesses very similar TS structures. Figure 4b and c depicts the TS structures on the Rh-step and the Rh-kink, respectively. At the TSs, the O is at the bridge site of a step-edge, and the C atom sits on the fcc site of the terrace near the step. It is obvious that there are five atoms involved in bonding with the TS complex, while it is only four on flat surfaces. The important structural parameters for the TSs are listed in Table 4. These types of TS structures on steps or kinks are similar to N_2 and NO dissociation on Ru-steps, as calculated by Dahl et al.¹⁹ and Hammer.²² We also noticed that the C–O distances at the TSs are longer, ranging from 2.09 to 2.5 Å (Table 4) as compared to those on the flat surfaces, which strongly implies that the TSs are “late” and are close to the FSs.

To find the most likely FS for CO dissociation on the defects, we have calculated individual C and O chemisorption energies at several possible sites after dissociation, including flat surfaces, considering that flat surfaces are always available. Our results are summarized as follows: (i) On both metals, the C atom is always more stable on the flat surfaces as compared to the fcc hollow site near the step (the bonding site of C at the TS). Therefore, $E_{\text{ad}}(\text{C})$ on the (111) surface is taken as the FS chemisorption energy on both Rh and Pd. (ii) On the Rh-step and the Rh-kink, the bridge site of the step-edge (the EB or KB site in Figure 1) is a more stable site for O atom chemisorption as compared to that on the flat surface. Thus, the O atom on the bridge site of the step-edge is taken as the FS for the O atom (on the Rh-step, $E_{\text{ad}}(\text{O}) = 4.99$ eV; on the Rh-kink, $E_{\text{ad}}(\text{O}) = 4.97$ eV; on Rh(111), $E_{\text{ad}}(\text{O}) = 4.78$ eV). (iii) On all Pd surfaces, the O atom is more stable on Pd(111) than that on the bridge site of the step-edge. Therefore, $E_{\text{ad}}(\text{O})$ on Pd(111) (4.39 eV) is taken as the FS energy for the O atom.

The reaction barriers for $\text{CO} \leftrightarrow \text{C} + \text{O}$ on the steps and the kinks of Rh and Pd were then calculated and listed in Table 3. It is interesting to find that both CO dissociation barriers and C

+ O association reaction barriers are remarkably reduced on the defects (Table 3). The magnitude of reduction is more than 0.6 eV on Rh, and up to 1.3 eV on Pd. Considering that the CO dissociation barriers are so low on the defects (0.2–0.3 eV on Rh, 0.4–0.6 eV on Pd), we expect that CO can dissociate even on Pd at a normal temperature, for example, 500 K. This might be reason for the experimental observation for the CH_4 formation from $\text{CO} + \text{H}_2$ even on late 4d and 5d metals: CO dissociates on defects first, followed by hydrogenation of reactions. It should be mentioned that CO can dissociate on the flat surface of earlier metals, such as Ru(0001) ($E_{\text{a}}^{\text{dis}} = 0.55$ eV at $1/4$ ML). It is obvious that the effect of the steps on the reactivity turns out to be more important at the late transition metals (we will discuss this later).

4. Insight into the Structure-Sensitivity of Catalytic Reactions

As discussed above, on different sites of a metal surface, the barrier of a reaction can vary significantly or be quite constant. Recent DFT calculations of Eichler⁵⁰ showed that the preexponential factor does not change significantly from surface to surface. Thus, the surface structure-sensitivity or -insensitivity is much related to the reaction barrier, and to understand how the reaction barrier is affected by the surface structure is crucial as to predict the surface structure-sensitivity. In this section, some qualitative understanding in heterogeneous catalysis will be first introduced. We then employ a more quantitative method to pinpoint individual energy terms in a reaction barrier. On the basis of this quantitative analysis, the physical origin of the surface structural effect will be discussed.

4.1. A Qualitative Understanding: Electronic and Geometrical Effects. In heterogeneous catalysis, two effects, the electronic and geometrical effects, have been used to understand qualitatively the activity of a catalyst for reactions. First, the electronic effect, for example, the change of work function at different surfaces, can affect the adsorbate chemisorption energy. Consequently, catalytic reactions may be facilitated or hindered by the change of the chemisorption as shown in our recent paper and others: It was found that the dissociation barrier is a linear function of the total chemisorption energy of dissociation products.^{30a} Second, the geometrical effect can affect the reaction pathway. Somorjai² suggested that a catalytic reaction that occurs at low coordinated sites, such as an atop or bridge site, is likely to be structure-insensitive, and the reaction's concentrations do not change markedly from surface to surface. On the contrary, the reaction that occurs at high coordinated sites is likely to be structure-sensitive. Applying these two effects to understand the reactions we have studied, we obtained some useful hints. For instance, the adsorbates, such as CH_3 and O, generally increase their chemisorption energies on steps. This is mainly due to an upshift of the d band,^{48,49} which is the electronic effect. As for the geometrical effect, the $\text{CO} \leftrightarrow \text{C} +$

(46) (a) Bleakley, K.; Hu, P. *J. Am. Chem. Soc.* **1999**, *121*, 7644. (b) Zhang, C. J.; Hu, P.; Lee, M.-H. *Surf. Sci.* **1999**, *432*, 305. (c) Lynch, M.; Hu, P. *Surf. Sci.* **2000**, *458*, 1.

(47) Mortensen, J. J.; Hammer, B.; Norskov, J. K. *Surf. Sci.* **1998**, *414*, 315.

(48) (a) News, D. M. *Phys. Rev.* **1969**, *178*, 1123. (b) Hoffmann, R. *Rev. Mod. Phys.* **1988**, *60*, 601. (c) Hammer, B.; Norskov, J. K. *Surf. Sci.* **1995**, *343*, 211.

(49) (a) Shustorovich, E.; Baetzold, R. C.; Muetterties, E. L. *J. Phys. Chem.* **1983**, *87*, 1100. (b) Hu, P.; King, D. A.; Lee, M.-H.; Payne, M. C. *Chem. Phys. Lett.* **1995**, *246*, 73.

(50) Eichler, A. *Surf. Sci.* **2002**, *498*, 314.

O reaction can be considered as a process requiring a high coordinated site for its TS geometry, and the $\text{CH}_4 \leftrightarrow \text{CH}_3 + \text{H}$ can be considered as a reaction with a low coordination site. Indeed, $\text{CO} \leftrightarrow \text{C} + \text{O}$ is highly structure-sensitive. However, there are some limitations in this simple argument. It is not completely correct to state that the $\text{CH}_4 \leftrightarrow \text{CH}_3 + \text{H}$ is structure-insensitive. In fact, the forward and reverse reactions of $\text{CH}_4 \leftrightarrow \text{CH}_3 + \text{H}$ are quite different with respect to the structure-sensitivity.

It is obvious that the above argument, due to its simplicity, does not provide a comprehensive picture of the structural effect on catalytic reactions. We believe that the following two questions need to be answered to provide a real insight into the structure-sensitivity. (i) Why is the reaction type (a dissociation or association reaction) important to the structure-sensitivity? (ii) What are the individual contributions of the electronic effect (defined as E) and the geometrical effect (defined as G) to the reaction barrier? Without knowing these, it is very difficult to predict whether a reaction is structure-sensitive or not, because there are four possible combinations, that is, ($E+$, $G+$), ($E-$, $G-$), ($E+$, $G-$) and ($E-$, $G+$), where $E+$ ($E-$) means that the electronic effect reduces (increases) the barrier and $G+$ and $G-$ are defined in a similar way.

4.2. Barrier Decomposition: A Quantitative Understanding. To answer the above questions, we have utilized the following energy decomposition method (also see our previous work, ref 30a,b) to analyze the reaction barriers. For a general reaction of $\text{AB} \leftrightarrow \text{A} + \text{B}$ starting from an AB molecule in the gas phase to the adsorbed A and B on surfaces (A and B represent atoms or fragments), one can write the dissociation barrier, E_a^{dis} , as (Figure 3):

$$E_a^{\text{dis}} = E_g^{\text{bond}} - E^{\text{TS}} \quad (1)$$

where E_g^{bond} is the A–B bond energy in the gas phase, and E^{TS} is the total chemisorption energy of A and B at the TS. Because catalytic reactions on metal surfaces generally belong to the “late TS” reactions, E^{TS} can be further decomposed into three terms (Figure 3):

$$E^{\text{TS}} = E_A^{\text{TS}} + E_B^{\text{TS}} - E_{\text{int}}^{\text{TS}} \quad (2)$$

where E_A^{TS} is the chemisorption energy of A at the TS geometry without B; E_B^{TS} is defined in a similar way; and $E_{\text{int}}^{\text{TS}}$ is a quantitative measure of the interaction between A and B at the TS. It is usually a positive energy term due to the repulsive nature between A and B at the TS geometry in heterogeneous catalysis. Thus, by combining eqs 1 and 2, we arrive at

$$E_a^{\text{dis}} = E_g^{\text{bond}} - E^{\text{TS}} = E_g^{\text{bond}} - (E_A^{\text{TS}} + E_B^{\text{TS}}) + E_{\text{int}}^{\text{TS}} \quad (3)$$

Equation 3 suggests that the dissociation barrier (E_a^{dis}) consists of three parts: (i) E_g^{bond} , the bonding energy of AB in the gas phase; (ii) E_A^{TS} and E_B^{TS} , the individual product (A, B) adsorption energies at the TS; and (iii) $E_{\text{int}}^{\text{TS}}$, the interaction energy between A and B at the TS. In a similar way, the association barrier can be written as the energy difference between the TS and the FS:

$$E_a^{\text{as}} = E^{\text{FS}} - E^{\text{TS}} = (E_A^{\text{FS}} + E_B^{\text{FS}}) - (E_A^{\text{TS}} + E_B^{\text{TS}}) + E_{\text{int}}^{\text{TS}} \quad (4)$$

Table 5. The Decomposition of the TS Chemisorption Energy (E^{TS}) of $\text{CH}_4 \rightarrow \text{CH}_3 + \text{H}$ and $\text{CO} \rightarrow \text{C} + \text{O}$ on Rh(111) and the Rh-Step (see Figure 3 and Eqs 1–4 for the Meaning of All of the Symbols)^a

$\text{CH}_4 \rightarrow \text{CH}_3 + \text{H}$		E_{CH_3}	E_{H}	ΣE	E_{int}	E_a^{dis}	E_a^{as}
Rh(111)	TS	1.59	2.75	4.34	0.20	0.67	0.65
	FS	1.88	2.92	4.80	0		
Rh-step	TS	1.80	2.85	4.65	0.16	0.32	0.59
	FS	2.16	2.92	5.10	0		
$\text{CO} \rightarrow \text{C} + \text{O}$		E_{O}	E_{C}	ΣE	E_{int}	E_a^{dis}	E_a^{as}
Rh(111)	TS	4.15	7.02	11.17	1.11	1.17	1.84
	FS	4.78	7.12	11.90	0		
Rh-step	TS	4.59	6.81	11.40	0.47	0.30	1.18
	FS	4.99	7.12	12.11	0		

^a For comparison, the chemisorption energies of the individual products, say CH_3 and H in the $\text{CH}_4 \rightarrow \text{CH}_3 + \text{H}$ reaction, C and O in the $\text{CO} \leftrightarrow \text{C} + \text{O}$ reaction, at the FSs are also listed. $\Sigma E = E_{\text{CH}_3} + E_{\text{H}}$ or $E_{\text{O}} + E_{\text{C}}$ in each reaction, respectively. In the gas phase, the C–H bonding energy of CH_4 is calculated to be 4.81 eV, and the C–O bonding energy of CO is 11.23 eV. All of the energies are in eV.

where E_A^{FS} and E_B^{FS} are the FS chemisorption energies of A and B, respectively. The interaction energy of A and B at the FS, that is, $E_{\text{int}}^{\text{FS}}$, is not included in eq 4. This is because under the reaction condition we studied (low coverages), $E_{\text{int}}^{\text{FS}}$ is normally zero: a large separation between A and B ensures no repulsive interaction between them.

Because all of the TSs we studied are late TSs, E_A^{TS} and E_B^{TS} reflect largely the A and B bonding ability on the metal surface. In other words, E_A^{TS} and E_B^{TS} are quite close to their FS counterparts, E_A^{FS} and E_B^{FS} . It is thus expected that $E_A^{\text{TS}} + E_B^{\text{TS}}$ is by and large determined by the local electronic effect of metals. The interaction energy, $E_{\text{int}}^{\text{TS}}$, is usually an energy cost due to the repulsive nature between A and B at the late TS. The $E_{\text{int}}^{\text{TS}}$ consists mainly of two parts: (i) the *bonding competition*, which is caused by A and B sharing bonding with surface atoms;^{29,30,46} and (ii) the *direct Pauli repulsion* between A and B. Both are closely related to the TS structure.⁴⁷ Thus, $E_{\text{int}}^{\text{TS}}$ is a quantitative measure of the geometrical effect on catalytic reactions.

We used eq 2 to decompose the E^{TS} of the $\text{CH}_4 \leftrightarrow \text{CH}_3 + \text{H}$ and $\text{CO} \leftrightarrow \text{C} + \text{O}$ reactions on Rh(111) and the Rh-step. The individual energy components are listed in Table 5, and the FS chemisorption energies are also listed for comparison. From Table 5, one can see how the surface structure affects the reaction barriers:

(i) For CH_4 dissociation, the barrier reduction (about 0.3 eV) from the flat surface to the step is due to the increase of $E_{\text{CH}_3}^{\text{TS}} + E_{\text{H}}^{\text{TS}}$ (ΣE^{TS}), which is the local electronic effect ($E_{\text{int}}^{\text{TS}}$'s are almost identical on these two surfaces). For dissociation reactions, the barrier reduction on steps should be generally true because steps always bond adsorbates more strongly (ΣE^{TS} increase) and $E_{\text{int}}^{\text{TS}}$ on steps is not lower than that on flat surfaces (the TS geometry on steps is similar to that on flat surfaces, if not energetically better). For the association reaction of $\text{CH}_3 + \text{H} \rightarrow \text{CH}_4$, although $E_{\text{CH}_3}^{\text{TS}} + E_{\text{H}}^{\text{TS}}$ on the step increases by ~ 0.3 eV, $E_{\text{CH}_3}^{\text{FS}} + E_{\text{H}}^{\text{FS}}$ also increases by ~ 0.3 eV as compared to their counterparts on the flat surface. Therefore, E_a^{as} has almost no change from the flat surface to the step considering that the $E_{\text{int}}^{\text{TS}}$'s are similar on these two surfaces.

(ii) For CO dissociation, $E_C^{\text{TS}} + E_O^{\text{TS}}$ on the step is about 0.23 eV larger than that on the flat surface (the electronic effect), and, remarkably, $E_{\text{int}}^{\text{TS}}$ decreases from 1.11 eV on the flat surfaces to 0.47 eV on steps. In total, E_a^{dis} on the step is 0.87 eV smaller than that on the flat surface. This large reduction of E_a^{dis} consists of two components: the electronic effect (0.23 eV) and the geometrical effect (0.64 eV). The geometrical effect is obviously much more important. For the association reaction of $\text{C} + \text{O} \rightarrow \text{CO}$, $E_C^{\text{FS}} + E_O^{\text{FS}}$ on the step is also 0.21 eV larger than that on the flat surface. Thus, the electronic effect stabilizes the TS and the FS in a similar magnitude, the same as that in the $\text{CH}_4 \leftrightarrow \text{CH}_3 + \text{H}$ reaction. Therefore, the reduction of E_a^{as} (eq 4) on the step is mainly caused by the large decrease in $E_{\text{int}}^{\text{TS}}$, the geometrical effect.

The barrier-decomposition results can be summarized as follows. First, the local electronic effect stabilizes the TS and the FS in a similar magnitude, which is not surprising, considering that the catalytic reactions on metal usually possess late TS. As a result, it always plays a positive role in reducing the dissociation barrier (eq 3), but little role in reducing the association barrier (eq 4). It should be mentioned that the magnitude of the local electronic effect on the dissociation reaction is found to be small, ~ 0.3 eV for both CH_4 and CO dissociations. Second, the geometrical effect, if it plays a role, can reduce both the dissociation and the association reaction (no role in $\text{CH}_4 \leftrightarrow \text{CH}_3 + \text{H}$, a significant role in $\text{CO} \leftrightarrow \text{C} + \text{O}$). The magnitude of the geometrical effect can be quite large, for example, 0.64 eV in the $\text{CO} \leftrightarrow \text{C} + \text{O}$ reaction.

4.3. Origin and General Trends of the Geometrical Effect.

Because the contribution of the geometrical effect on both dissociation and association reactions can be significant, in this subsection we will focus on the origin of this effect and reveal its general trends. As mentioned above, $E_{\text{int}}^{\text{TS}}$ contains mainly two components, that is, the energy cost from the bonding competition effect and the direct Pauli repulsion. The Pauli repulsion is by and large determined by the distance between two reactants. It is noticed that, say in $\text{CO} \leftrightarrow \text{C} + \text{O}$ on Rh surfaces, because the C–O distances at the TSs on flat Rh(111) (1.87 Å) and the Rh-step (2.09 Å) are not so different (as compared to the 1.13 Å of the CO molecule), the Pauli repulsion contributions to $E_{\text{int}}^{\text{TS}}$ for the reaction on flat Rh(111) and that on the Rh-step should be quite similar. Therefore, the major difference of $E_{\text{int}}^{\text{TS}}$ between the flat Rh(111) and the Rh-step, that is, the geometrical effect, should originate from the variation of the bonding competition effect from the flat surface to the step.

We have done the following analysis on an $\text{A} + \text{B}$ coadsorption system to quantitatively investigate the magnitude of the bonding competition effect. First, we define a *standard bonding competition energy* (E_{int}^0) for the $\text{A} + \text{B}$ coadsorption system:

$$E_{\text{int}}^0 = E_A + E_B - E_{\text{A+B}} \quad (5)$$

where $E_{\text{A+B}}$ is the total chemisorption energy of $\text{A} + \text{B}$ coadsorption in which A and B are placed at two neighboring hcp sites in a $p(2 \times 2)$ unit cell (thus they share surface atoms), with the positions of A and B corresponding to their individual optimized adsorption positions; E_A (E_B) is the individual chemisorption energy of A (B). In such a structure, the distance between A and B is about 2.7 Å, at which the direct Pauli

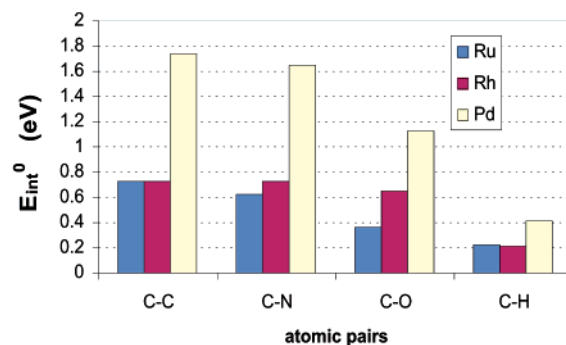


Figure 5. The calculated E_{int}^0 for different atomic pairs on Ru(0001), Rh(111), and Pd(111) using eq 5.

repulsion between A and B is believed to be negligible. Thus, E_{int}^0 measures mainly the bonding competition effect between A and B. We have calculated E_{int}^0 for different atomic pairs, C–C, C–N, C–O, C–H on the 4d metals Ru(0001), Rh(111), and Pd(111). The values are shown in Figure 5. Two general trends can be seen in Figure 5: (i) For each pair, the E_{int}^0 increases from the left to the right in the periodical table, $\text{Pd} > \text{Rh} > \text{Ru}$. (ii) As the adsorbate valency decreases, the E_{int}^0 decreases, $\text{C–C} > \text{C–N} > \text{C–O} > \text{C–H}$.

It is interesting to note that the E_{int}^0 of the C–O pair has a value of 1.13 eV on Pd, which is almost twice as big as that on Rh(111) (0.65 eV). This is well consistent with what we have found for the barrier reduction in CO dissociation from the flat surfaces to the steps: on Pd it is 1.30 eV, which is nearly twice as big as that on Rh (0.70 eV). Therefore, the larger barrier reduction on Pd as compared to Rh can be attributed to its larger E_{int}^0 , a consequence of the bonding competition effect. For the $\text{CH}_4 \leftrightarrow \text{CH}_3 + \text{H}$ reaction, we can use Figure 5 to understand why the $E_{\text{int}}^{\text{TS}}$ of $\text{CH}_4 \leftrightarrow \text{CH}_3 + \text{H}$ is so small, only 0.2 eV (Table 5). Both CH_3 and H only have one valency, and thus they do not induce a large bonding competition effect.

4.4. Where a Catalytic Reaction Should Occur: A General Discussion. From the above results, the following rules can be generalized regarding where a catalytic reaction should occur: (i) Dissociation reactions always occur preferentially on surface defects. (ii) Association reactions with *higher-valency* reactants are more likely to occur on surface defects than those with lower-valency reactants. (iii) Association reactions on the *later transition metals*, such as Pd and Pt, are more structure-sensitive than those on the earlier transition metals.

These rules can be used to explain why ammonia synthesis is highly structure-sensitive: one of the most important elementary steps in ammonia synthesis is the N_2 dissociation in which the product, N atom, possesses a high valency. According to the rules above, the N_2 dissociation should be structure-sensitive (prefer to occur on steps), which is consistent with experiment. The fact that the Fischer–Tropsch synthesis, for example, on Co, is structure-sensitive may also be explained. Our recent calculations have shown that the barriers for C/C coupling reactions on Ru, such as $\text{C} + \text{CH}$ and $\text{C} + \text{CH}_2$ in which one of the reactants (i.e., C) possess high valency, are much lower on steps than those on flat surfaces.⁵² For the same reason, association reactions involving H atoms (small valency), that is, hydrogenation reactions, are structure-insensitive. In other

(51) Hammer, B. *J. Catal.* **2001**, *199*, 171.

(52) Liu, Z.-P.; Hu, P. *J. Am. Chem. Soc.* **2002**, *124*, 11568.

words, the barriers of hydrogenation reactions on flat surfaces will be similar to those on steps.

Finally, it is interesting to discuss the structure effect of CO oxidation on metals. As mentioned in the Introduction, CO oxidation on transition metals seems not to be very sensitive to the surface structure change. The reasons are as follows: First, it belongs to the association reaction, which is quite insensitive to the electronic effect. Second, the bonding competition between CO and O atom was found to be quite small because of its TS geometry.^{30b} Therefore, the barriers of CO oxidation on flat surfaces and steps of the same metal will be similar. For example, the barrier reported for $\text{CO} + \text{O} \rightarrow \text{CO}_2$ on Pd(111) at $1/4$ ML is 0.93 eV by Zhang and Hu,²⁵ and on Pd-step the barrier was reported to be 1.0 eV by Hammer.⁵¹

5. Conclusions

This work represents one of the attempts to obtain a comprehensive picture of the surface structure effect on catalytic reactions. Two types of reactions, $\text{CH}_4 \leftrightarrow \text{CH}_3 + \text{H}$ and $\text{CO} \leftrightarrow \text{C} + \text{O}$, on two transition metal surfaces were chosen as model systems aiming to address in general where a catalytic reaction should occur. The dissociations of $\text{CH}_4 \rightarrow \text{CH}_3 + \text{H}$ and $\text{CO} \rightarrow \text{C} + \text{O}$ and their reverse reactions on flat, stepped, and kinked Rh and Pd surfaces were studied in detail. The reaction pathways and reaction barriers were calculated. The following conclusions regarding chemisorption energies of reactants and reaction barriers are obtained:

(i) The H chemisorption energy on the flat Rh(111) is 2.92 eV, which is very similar to the H chemisorption energies on the Rh-step and the Rh-kink. On the flat Pd(111), Pd-step, and Pd-kink, the H chemisorption energies are also similar (3.05 eV).

(ii) The CH_3 chemisorption energy on the flat Rh(111) is 1.88 eV, and on the Rh-step and the Rh-kink the chemisorption energies are identical (2.16 eV) and slightly larger than that on the flat surface. On Pd surfaces, the CH_3 chemisorption energy is in the following order: Pd-step (2.01 eV) > Pd-kink (1.88 eV) > Pd(111) (1.78 eV).

(iii) The CH_4 dissociation barrier on the flat Rh(111) is 0.67 eV. The barriers on the Rh-step and Rh-kink are similar (0.32 and 0.20 eV, respectively), but significantly lower than that on the flat Rh(111). Similarly, on Pd the CH_4 dissociation barrier is reduced by ~ 0.3 eV from the flat surface (0.66 eV) to the steps (0.38 eV) and kinks (0.41 eV).

(iv) The CO dissociation barrier on the flat Rh(111) is 1.17 eV, and it is dramatically reduced on the Rh-step (0.3 eV) and the Rh-kink (0.21 eV). On Pd(111), the CO dissociation barrier is very high (1.87 eV). Again, the barriers on the Pd-step (0.57 eV) and the Pd-kink (0.38 eV) are much lower than that on the flat Pd(111). The TSs for CO dissociation on the flat surfaces involve four metal atoms, and the C and O share bonding with one metal atom, while the TSs involve five atoms on steps and kinks with no metal atoms being shared.

(v) The association barriers of $\text{CH}_3 + \text{H}$ on the flat Rh(111), the Rh-step, and the Rh-kink are very similar (0.65, 0.59, and 0.49 eV, respectively). They are also similar to that on the Pd(111), the Pd-step, and the Pd-kink (0.68, 0.63, 0.53 eV, respectively). In contrast, the association barriers of the $\text{C} + \text{O}$ on the flat surfaces are very different from those on steps and kinks. On the flat Rh(111) and Pd(111), the barriers of $\text{C} + \text{O}$ are 1.84 and 1.98 eV, respectively. On the Rh-step and Rh-kink, the barriers are similar (1.18 and 1.09 eV, respectively), but are significantly lower than that on the flat Rh(111). This is also true for the barriers on the Pd-step and Pd-kink (0.68 and 0.49 eV, respectively).

On the basis of our reaction barrier decomposition, we obtain the following understanding of the barrier on different sites:

(i) For CH_4 dissociation, the reduction of the barrier by ~ 0.3 eV on the steps as compared to on the flat surfaces is mainly due to the local electronic effect. The geometrical effect plays little role in affecting the barriers. Because of the barrier reduction on steps, steps are always favored for CH_4 dissociation. On the other hand, there is essentially no difference in barrier for the association reaction of $\text{CH}_3 + \text{H}$ on the flat surfaces and defects, because the extent of the local electronic effect on the initial state is almost the same as that on the TS and no geometrical effect exists.

(ii) For the $\text{CO} \rightarrow \text{C} + \text{O}$ reaction, the geometrical effect is more important than the local electronic effect in reducing the barrier from the flat surfaces to the defects. The electronic effect is ~ 0.3 eV, while the geometrical effect is more than 0.6 eV. Because of a large amount of barrier decrease on the steps and kinks as compared to on the flat surfaces, defects are much more favored for CO dissociation. In contrast to the $\text{CH}_3 + \text{H}$ reaction, the $\text{C} + \text{O}$ association reaction also preferentially occurs on steps and kinks due to the geometrical effect.

Finally, we arrive at some simple rules with respect to where a reaction should occur as follows:

(i) Defects such as steps are always favored for dissociation reactions as compared to flat surfaces. In other words, dissociation reactions are structure-sensitive.

(ii) Association reactions can be either structure-sensitive or structure-insensitive. The structure-sensitivity, that is, where a reaction should occur, is largely related to the bonding competition effect, which is determined by the reactant and metal valency. First, reactions with high valency reactants are more structure-sensitive, as compared to reactions with low valency reactants. Second, the reaction on the early transition metals is less structure-sensitive than that on the late transition metals.

Acknowledgment. We gratefully acknowledge the UKCP for computing time in T3E and the Supercomputing Center in Ireland for computing time in IBM-SP. Z.-P.L. thanks The Queen's University of Belfast for a studentship.

JA0207551